FERMILAB-CONF-17-335-E
ACCEPTED

Latest Results from MINOS and MINOS+

Simon De Rijck, for the MINOS and MINOS+ Collaborations
University of Texas at Austin, Department of Physics, 2515 Speedway, C1600, Austin, TX 78712-1192

E-mail: simonderijck@gmail.com

Abstract. The MINOS and MINOS+ experiments collected accelerator beam neutrino and antineutrino data for 11 years corresponding to peak energies of 3 GeV and 6 GeV, respectively, over a baseline of 735 km. These proceedings report on new limits and constraints set by MINOS and MINOS+ in and beyond the standard three-flavor paradigm. The atmospheric neutrino mass splitting in the three-flavor model is measured to be $(2.42 \pm 0.09) \times 10^{-3}\,\mathrm{eV}^2$ for normal mass ordering and $-(2.48^{+0.09}_{-0.11}) \times 10^{-3}\,\mathrm{eV}^2$ for inverted mass ordering. Constraints are set on sterile neutrinos and antineutrinos in the four-flavor model by looking for sterile-driven ν_μ and $\overline{\nu}_\mu$ disappearance and sterile-driven ν_e and $\overline{\nu}_e$ appearance. A combination of the MINOS four-flavor ν_μ disappearance search and the Daya Bay and Bugey-3 four-flavor $\overline{\nu}_e$ disappearance searches excludes the parameter space allowed by LSND and MiniBooNE for $\Delta m^2_{41} < 0.8\,\mathrm{eV}^2$ at 90% C.L. The size of large extra dimensions is constrained to be smaller than 0.17 μm at 90% C.L. in the limit of a vanishing lightest active neutrino mass. Finally, a search for non-standard ν_e and $\overline{\nu}_e$ appearance in MINOS is presented.

1. Introduction

MINOS and MINOS+ are long baseline neutrino oscillation experiments that ran from 2005 through 2012 and 2013 through 2016, respectively. Charged Current (CC) and Neutral Current (NC) interactions of accelerator beam muon neutrinos from the Neutrinos at the Main Injector (NuMI) beam [1] at Fermilab are measured by two functionally identical detectors located on the NuMI beamline axis. Both detectors are magnetized tracking-sampling calorimeters built of iron plates interleaved with scintillator planes, the latter being read out using wavelength-shifting fibers coupled to multi-anode photomultiplier tubes. The Near Detector (ND) is located 1.04 km downstream of the NuMI target at Fermilab and has a 23.7 t fiducial (980 t total) mass. The Far Detector (FD) is located 735 km downstream of the NuMI target in Soudan, Minnesota and has a 4.2 kt fiducial (5.4 kt total) mass [2].

The magnetic horns in NuMI allow to operate the beam in either ν_μ or $\overline{\nu}_\mu$ mode. During the MINOS era, NuMI provided a beam with a peak neutrino energy of 3 GeV corresponding to an exposure of 10.71×10^{20} protons-on-target (POT) when operating in ν_μ mode and 3.36×10^{20} POT in $\overline{\nu}_\mu$ mode. The peak neutrino energy increased to 6 GeV for MINOS+, with NuMI providing an exposure of 5.80×10^{20} POT in ν_μ mode during the first two years of running. The analysis of the final year of MINOS+ beam data is ongoing.

MINOS was originally designed to perform precision measurements of the atmospheric neutrino oscillation parameters in the standard three-flavor model, Δm^2_{32} and θ_{23}, by observing muon neutrino disappearance occurring along the FD baseline. The shift to higher neutrino

This document was prepared by [COLLABORATION NAME] using the resources of the Fermi National Accelerator Laboratory (Fermilab), a U.S. Department of Energy, Office of Science, HEP User Facility. Fermilab is managed by Fermi Research Alliance, LLC (FRA), acting under Contract No. DE-AC02-07CH11359.

energies in MINOS+, away from the FD three-flavor oscillation minimum at 1.5 GeV, motivates searches beyond the standard three-flavor model, including searches for sterile neutrinos in the four-flavor model, large extra dimensions, and non-standard interactions.

2. Standard Three-Flavor Oscillation

In the three-flavor oscillation paradigm, MINOS and MINOS+ employ CC ν_μ beam and atmospheric events to search for ν_μ disappearance in the FD, and CC ν_e beam events to search for ν_e appearance in the FD. An update to the MINOS result [3] was performed by adding the first two years of MINOS+ beam exposure and an extra year of atmospheric events to the MINOS dataset [4]. The FD reconstructed beam ν_μ energy spectrum is shown in Fig. 1a and the 68% and 90% C.L. contours are compared to results from other experiments in Fig. 1b. To date, MINOS and MINOS+ provide one of the best limits on Δm^2_{32}, with $\Delta m^2_{32} = (2.42 \pm 0.09) \times 10^{-3}\,\mathrm{eV}^2$ for normal mass ordering and $\Delta m^2_{32} = -(2.48^{+0.09}_{-0.11}) \times 10^{-3}\,\mathrm{eV}^2$ for inverted mass ordering.

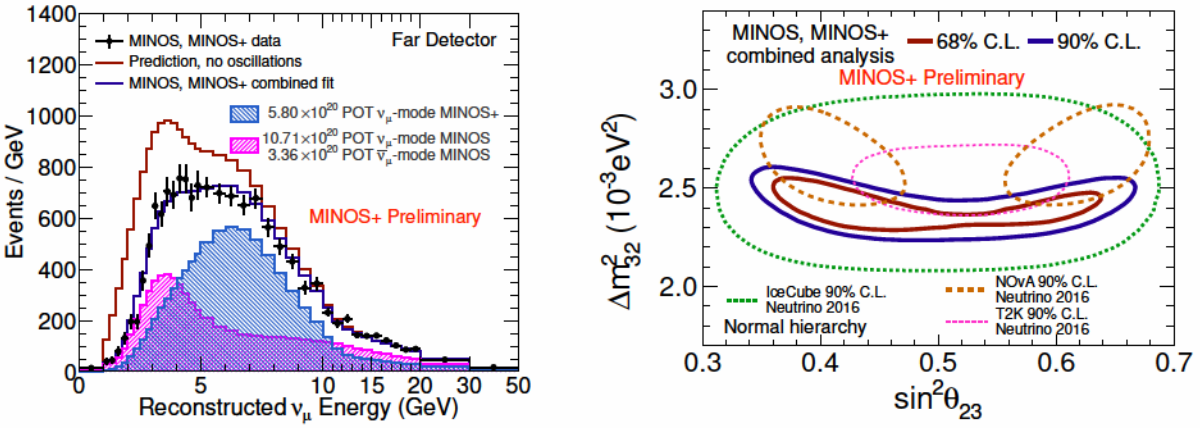

(a) (b)

Figure 1: Updated standard oscillation result. (a) The reconstructed beam ν_μ energy spectrum for MINOS and MINOS+ FD selected events. Predictions are shown for no oscillations (red line) and for oscillations at the MINOS and MINOS+ combined best fit (blue line), with the MINOS (hashed magenta) and MINOS+ (hashed blue) contributions shown separately. (b) The 68% (red line) and 90% (blue line) C.L. contours resulting from a fit to 48.67 kt-yrs of atmospheric data combined with disappearance and appearance data from the MINOS beam and disappearance data from the MINOS+ beam during the first two years of operation. The combined MINOS and MINOS+ contours are compared with the 90% C.L. limits of NOνA [5], T2K [6], and IceCube DeepCore [7] presented at Neutrino 2016.

3. Sterile Neutrinos in the Four-Flavor Model

As precision experiments, MINOS and MINOS+ employ their data to look for discrepancies from the three-flavor paradigm that could be accounted for by small modifications to the standard three-flavor model. One such scenario adds one sterile neutrino state that can mix with the three active neutrino states. This minimal extension to the three-flavor model requires three additional mixing angles, θ_{14}, θ_{24}, and θ_{34}, one additional independent mass splitting, Δm^2_{41}, and two additional CP-violating phases, δ_{14} and δ_{24}.

3.1. Sterile Neutrino Search through Disappearance

MINOS and MINOS+ are sensitive to θ_{24} by searching for CC ν_μ disappearance and sterile neutrino appearance, the latter showing itself as a deficit of NC ν_i ($i = e,\mu,\tau$) events compared to the three-flavor expectation. Unlike in the three-flavor model, significant oscillation along the ND baseline is possible. To account for this, the ratio of the measured FD and ND neutrino energy spectra, the Far-over-Near ratio, is compared to the four-flavor predictions. The Far-over-Near ratio for MINOS and MINOS+ selected CC events is shown in Fig. 2a.

MINOS and MINOS+ put constraints on θ_{24} over many orders of magnitude of Δm^2_{41}. No evidence for a sterile neutrino has been found [4, 8]. The combined MINOS and MINOS+ 90% and 95% C.L. Feldman-Cousins corrected contours are compared to results from other experiments in Fig. 2b.

A combination, employing the CL_s technique, of the MINOS disappearance result [8], placing limits on θ_{24}, and the $\overline{\nu}_e$ disappearance results of Daya Bay [9] and Bugey-3 [10], both placing limits on θ_{14}, allows a direct comparison with ν_e appearance results in the $(\sin^2 2\theta_{\mu e}, \Delta m^2_{41})$ plane, where

$$\sin^2 2\theta_{\mu e} = \sin^2 2\theta_{14} \sin^2 \theta_{24}. \quad (1)$$

The combined result, shown in Fig. 3a, excludes the LSND and MiniBooNE allowed regions for $\Delta m^2_{41} < 0.8\,\mathrm{eV}^2$ at 90% C.L. [11].

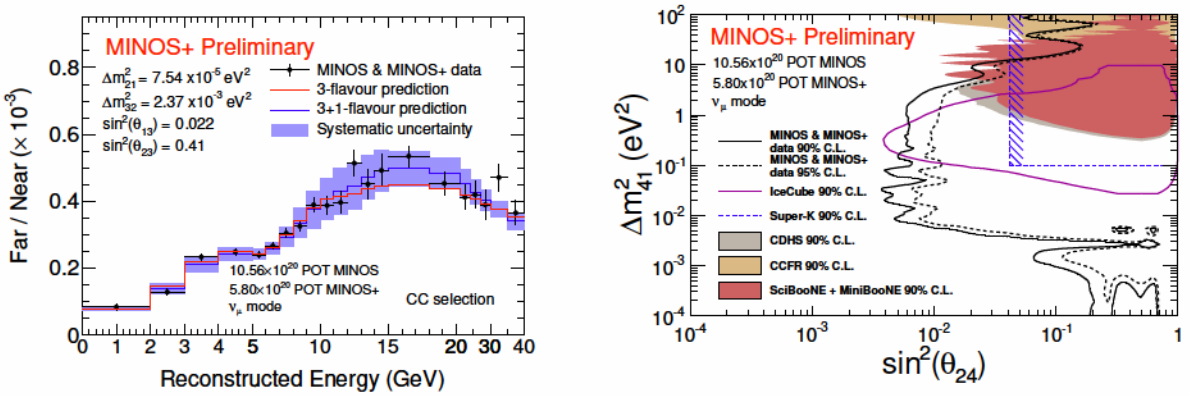

(a) (b)

Figure 2: Constraining the four-flavor model with ν_μ disappearance. (a) The Far-over-Near ratio of observed MINOS and MINOS+ ν_μ CC beam events. The four-flavor best fit result is shown in blue with parameters $\Delta m^2_{41} = 24.01\,\mathrm{eV}^2$, $\Delta m^2_{32} = 2.512 \times 10^{-3}\,\mathrm{eV}^2$, $\theta_{23} = 0.917$, $\theta_{24} = 0.294$, and $\theta_{34} = 2.06 \times 10^{-11}$. (b) The combined MINOS and MINOS+ 90% (black line) and 95% (dashed black line) C.L. Feldman-Cousins corrected contours in the $(\sin^2 \theta_{24}, \Delta m^2_{41})$ plane using CC ν_μ disappearance and searching for a deficit in NC events. The combined MINOS and MINOS+ contours are compared to results from IceCube [12], Super-K [13], CDHS [14], CCFR [15], and SciBooNE + MiniBooNE [16].

3.2. Sterile Neutrino Search through ν_e Appearance

Through CC ν_e appearance in the FD, MINOS+ puts direct constraints on the four-flavor model in the $(\sin^2 2\theta_{\mu e}, \Delta m^2_{41})$ plane. The analysis utilizes an extended version of the framework developed for the MINOS three-flavor CC ν_e analyses [21], selecting only CC ν_e and $\overline{\nu}_e$

events above 6 GeV, away from the standard three-flavor oscillation minimum. The 90% C.L. contour based on the first year of MINOS+ beam data is shown in Fig. 3a.

3.3. Sterile Antineutrino Search through Disappearance

The ND and FD are magnetized, allowing separation of neutrinos and antineutrinos on an event-by-event basis. CC $\overline{\nu}_\mu$ events are selected from the MINOS beam data acquired during both $\overline{\nu}_\mu$ and ν_μ operations. Figure 3b compares the MINOS 90% C.L contour to results from other experiments. MINOS provides the strongest disappearance constraints for $\Delta\overline{m}^2_{41} < 0.5\,\mathrm{eV}^2$.

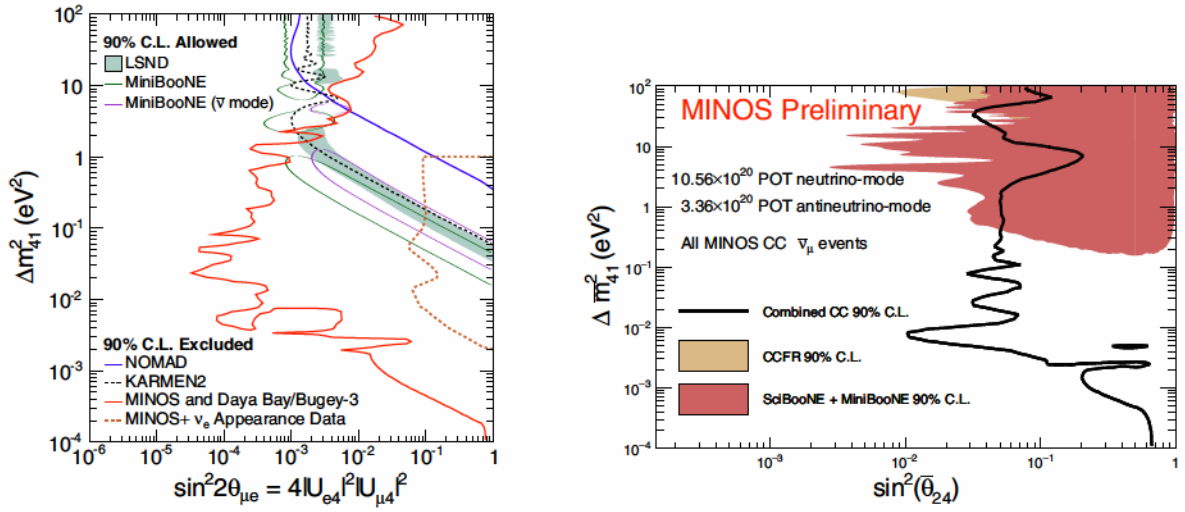

(a) (b)

Figure 3: Constraining the four-flavor model with ν_e appearance and antineutrinos. (a) The MINOS and Daya Bay/Bugey-3 combined 90% CL_s limit (red line) on $\sin^2 2\theta_{\mu e}$ and the 90% C.L. contour (dashed orange line) using ν_e and $\overline{\nu}_e$ appearance events collected during the first year of MINOS+ are compared to the LSND [17] and MiniBooNE [18] 90% C.L. allowed regions. The regions excluded at 90% C.L. by KARMEN2 [19] and NOMAD [20] are also shown. (b) The MINOS 90% C.L. Feldman-Cousins corrected contour in the $(\sin^2\overline{\theta}_{24}, \Delta\overline{m}^2_{41})$ plane using $\overline{\nu}_\mu$ disappearance.

4. Large Extra Dimensions

MINOS and MINOS+ also search for extra dimensions. In the Large Extra Dimension (LED) model of [22, 23, 24, 25], sterile neutrinos arise as Kaluza-Klein states in a large extra dimension compactified on a circle with radius R. These sterile neutrino states mix with the active neutrino states and thereby modify the neutrino oscillation probabilities. The effects of the large extra dimension are governed by R and the lightest active neutrino mass m_0.

Following the Far-over-Near ratio approach of the four-flavor search and in the limit of a vanishing m_0, MINOS beam data constrains R to be smaller than 0.45 µm [26], while adding MINOS+ beam data tightens the constraint to $R < 0.17$ µm at 90% C.L. [4]. Figure 4a shows the 90% C.L. contours based on MINOS beam data and combined MINOS and MINOS+ beam data.

5. Non-Standard Interactions

The oscillation probability observed in the FD would also be modified if neutrinos undergo non-standard interactions with matter when traveling from Fermilab to Minnesota. Such non-standard interactions would induce an additional term in the interaction Hamiltonian which can be parameterized by the coupling coefficients $\epsilon_{\alpha\beta}$ $(\alpha, \beta = \mathrm{e}, \mu, \tau)$,

$$H_{\mathrm{NSI}} = \sqrt{2} G_{\mathrm{F}} N_{\mathrm{e}} \begin{pmatrix} \epsilon_{\mathrm{ee}} & \epsilon^*_{\mathrm{e}\mu} & \epsilon^*_{\mathrm{e}\tau} \\ \epsilon_{\mathrm{e}\mu} & \epsilon_{\mu\mu} & \epsilon^*_{\mu\tau} \\ \epsilon_{\mathrm{e}\tau} & \epsilon_{\mu\tau} & \epsilon_{\tau\tau} \end{pmatrix}, \tag{2}$$

where G_{F} is the Fermi coupling constant and N_{e} is the electron density of the matter through which the neutrinos travel. The oscillation probabilities furthermore depend on three additional phases, $\delta_{\mathrm{e}\mu}$, $\delta_{\mathrm{e}\tau}$, and $\delta_{\mu\tau}$ [27, 28, 29, 30]. Employing ν_{e} and $\overline{\nu}_{\mathrm{e}}$ appearance events in the FD, MINOS has set constraints on $|\epsilon_{\mathrm{e}\tau}|$ as a function of $(\delta_{\mathrm{CP}} + \delta_{\mathrm{e}\tau})$ [31], as shown in Fig. 4b.

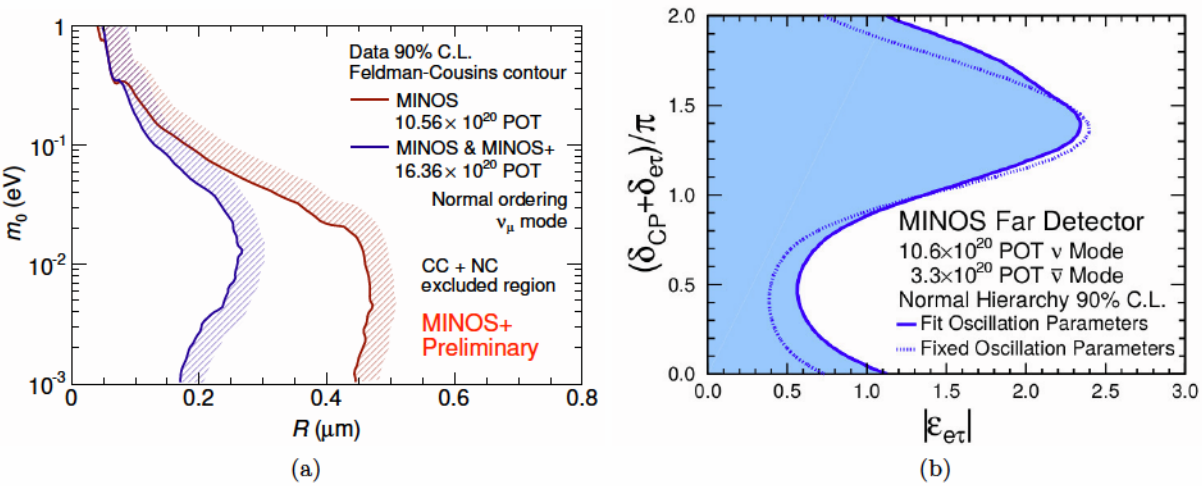

Figure 4: Constraining exotic models beyond the three-flavor paradigm. (a) Comparison of the 90% C.L. contour for the LED model, obtained using the Feldman-Cousins technique, based on 10.56×10^{20} POT MINOS data and the contour obtained when adding 5.80×10^{20} POT MINOS+ data. The large extra dimension size and the smallest neutrino mass are denoted as R and m_0, respectively. (b) The MINOS 90% C.L. contour in the $(|\epsilon_{\mathrm{e}\tau}|, \delta_{\mathrm{CP}} + \delta_{\mathrm{e}\tau})$ plane for normal neutrino mass ordering using ν_{e} and $\overline{\nu}_{\mathrm{e}}$ appearance events in the FD. The shaded areas to the left of the solid contours indicate the MINOS allowed regions where additional oscillation parameters, including the non-standard interaction parameters, were included in the fit. The dotted contours show the limits where the additional oscillation parameters were fixed.

6. Conclusions

Between observing the first atmospheric neutrino event in the MINOS FD on August 1, 2003, and collecting the last beam neutrino event on June 29, 2016, MINOS and MINOS+ collected 2.38×10^{21} POT of accelerator beam neutrino data and 60.9 kt-yrs of atmospheric neutrino data. The addition of the first two years of MINOS+ beam data to the MINOS beam dataset leads to one of the best measurements of the atmospheric mass splitting in the standard three-flavor

model, produces leading constraints over many orders of magnitude in the new mass splitting on sterile neutrino and antineutrino searches in the four-flavor model, and results in the strongest constraints on the size of large extra dimensions reported by a neutrino oscillation experiment. Inclusion of the final year of MINOS+ data will further improve our results in and beyond the three-flavor paradigm.

References

[1] Adamson P *et al.* (MINOS Collaboration) 2016 *Nucl. Instrum. Meth. A* **806** 279-306
[2] Michael D G *et al.* (MINOS Collaboration) 2008 *Nucl. Instrum. Meth. A* **596** 190-228
[3] Adamson P *et al.* (MINOS Collaboration) 2014 *Phys. Rev. Lett.* **112** 191801
[4] Evans J *New results from MINOS and MINOS+* Talk at the XXVII International Conference on Neutrino Physics and Astrophysics (Neutrino 2016), London, 2016
[5] Vahle P *New results from NOνA* Talk at the XXVII International Conference on Neutrino Physics and Astrophysics (Neutrino 2016), London, 2016
[6] Tanaka H *Status, recent results and plans for T2K* Talk at the XXVII International Conference on Neutrino Physics and Astrophysics (Neutrino 2016), London, 2016
[7] Koskinen D J *Atmospheric neutrino results from IceCube/DeepCore and plans for PINGU* Talk at the XXVII International Conference on Neutrino Physics and Astrophysics (Neutrino 2016), London, 2016
[8] Adamson P *et al.* (MINOS Collaboration) 2016 *Phys. Rev. Lett.* **117** 151803
[9] An F P *et al.* (Daya Bay Collaboration) 2016 *Phys. Rev. Lett.* **117** 151802
[10] Achkar B *et al.* (Bugey-3 Collaboration) 1995 *Nucl. Phys. B* **434** 503
[11] Adamson P *et al.* (MINOS and Daya Bay Collaborations) 2016 *Phys. Rev. Lett.* **117** 151801
[12] Aartsen M G *et al.* (IceCube Collaboration) 2016 *Phys. Rev. Lett.* **117** 0712801
[13] Abe K *et al.* (Super Kamiokande Collaboration) 2015 *Phys. Rev. D* **91** 052019
[14] Dydak F *et al.* (CDHS Collaboration) 1984 *Phys. Lett. B* **134** 281
[15] Stockdale I E *et al.* (CCFR Collaboration) 1984 *Phys. Rev. Lett.* **52** 1384
[16] Mahn K B M *et al.* (MiniBooNE and SciBooNE Collaborations) 2012 *Phys. Rev. D* **85** 032007
[17] Aguilar A *et al.* (LSND Collaboration) 2001 *Phys. Rev. D* **64** 112007
[18] Aguilar-Arevalo A *et al.* (MiniBooNE Collaboration) 2013 *Phys. Rev. Lett.* **110** 161801
[19] Armbruster B *et al.* (KARMEN Collaboration) 2002 *Phys. Rev. D* **65** 112001
[20] Astier P *et al.* (NOMAD Collaboration) 2003 *Phys. Lett. B* **570** 19
[21] Adamson P *et al.* (MINOS Collaboration) 2013 *Phys. Rev. Lett.* **110** 171801
[22] Dienes K R, Dudas E and Gherghetta T 1999 *Nucl. Phys. B* **557** 25
[23] Arkani-Hamed N, Dimopoulos S, Dvali G R and March-Russell J 2001 *Phys. Rev. D* **65** 024032
[24] Davoudiasl H, Langacker P and Perelstein M 2002 *Phys. Rev. D* **65** 105015
[25] Machado P A N, Nunokawa H and Zukanovich Funchal R 2011 *Phys. Rev. D* **84** 013003
[26] Adamson P *et al.* (MINOS Collaboration) 2016 *Phys. Rev. D* **94** 111101(R)
[27] Ganzalez-Garcia M C, Guzzo M M, Krastev P I, Nunokawa H, Peres O L G, Pleitez V, Valle J W F and Zukanovich Funchal R 1999 *Phys. Rev. Lett.* **82** 3202
[28] Friedland A, Lunardini C and Maltoni M 2004 *Phys. Rev. D* **70** 111301
[29] Friedland A and Lunardini C 2006 *Phys. Rev. D* **74** 033012
[30] Ohlsson T 2013 *Rep. Prog. Phys.* **76** 044201
[31] Adamson P *et al.* (MINOS Collaboration) 2017 *Phys. Rev. D* **95** 012005